Light-scattering study of slow and fast dynamics in a strong inorganic glass former

S. N. Yannopoulos
Institute of Chemical Engineering and High Temperature Chemical Processes, Foundation for Research and Technology–Hellas, P.O. Box 1414, GR-26500 Patras, Greece

G. N. Papatheodorou
Institute of Chemical Engineering and High Temperature Chemical Processes, Foundation for Research and Technology–Hellas, P.O. Box 1414, GR-26500, Patras, Greece
and Department of Chemical Engineering, University of Patras, GR-26500, Patras, Greece

G. Fytas
Institute of Electronic Structure and Laser, Foundation for Research and Technology–Hellas, P.O. Box 1527, GR-71110, Heraklion, Crete, Greece

(Received 17 May 1999)

The dynamic properties of glassy and liquid As_2O_3 are investigated over a wide temperature range, in both the microscopic and macroscopic time domains by Brillouin scattering (BS) and photon correlation spectroscopy (PCS). The two characteristic properties of sound propagation, velocity, and attenuation were found to exhibit considerable, although unexpected, changes very close to the glass transition temperature T_g. The high-frequency density fluctuations were quantitatively treated using a phenomenological formulation for the corresponding memory function, which considers both slow and fast processes. The obtained viscoelastic parameters were found to follow physically acceptable temperature dependencies. Both density and orientation autocorrelation functions show a very narrow distribution of relaxation times with a shape parameter close to 0.8. The peculiarities of the sound-velocity and the sound-absorption coefficient as well as the comparison between the PCS and the BS relaxation times confirmed the existence of two relaxation processes differing by 10 orders of magnitude near T_g. The difference in activation energies, for the fast process, between strong and fragile glasses is discussed on the basis of the stability of asymmetric double-well potentials over a relaxation period. Evidence is provided conforming to the two fluid model predictions, invoking long-range density fluctuations. Pseudotransformations of chemically and topologically ''acceptable'' structures seem to be the driving force for low-energy excitations in network bonded glasses. [S0163-1829(99)02446-7]

I. INTRODUCTION

In the past few years the inability of an adequate understanding of many features accompanying glass formation as well as the glassy state itself has become evident.[1] This incomplete knowledge concerns both dynamical and structural aspects of the amorphous materials. Older theoretical approaches and experimental techniques have been modified and new ones have been developed,[2] intending to shed more light on the mechanisms underlying the vitrification process in amorphous solids. The apparent similarity in the behavior of disordered systems with different chemical nature has been exploited by many phenomenological attempts. Universality arguments are frequently adopted when certain dynamical properties appear to follow similar behavior obeying the same law(s). Albeit a unique description of all salient features of the amorphous state is today not possible, the mode coupling theory[2(a)] (MCT) and the coupling scheme for relaxation appear to account for certain experimental findings regarding mainly the dynamic properties;[2(b)] although the former has been subjected to serious criticism.[3] Further, new information on the distribution of the primary relaxation times, the presence of fast dynamics associated with glass transition and the length scale dependence of the glass dynamics in confined geometry,[1(a)] enrich the phenomenology of the complex behavior of viscoelastic fluids.

The phenomenology of glass dynamics has emerged mainly from experiments on organic (molecular or macromolecular) glass formers, which mainly fall into the category of fragile glasses; a classification based on the rate of increase of fluidity with temperature. Alternatively, few experiments on strong glasses have appeared so far, revealing an additional fast process in the vicinity of T_g.[4(a),5] It is worth noticing that the interpretation of the fast dynamics by the MCT approach in Ref. 4(a) encounters problems when additional light scattering data[4(b)] are put in focus. It has also been stated that the fast β process of MCT cannot be seen in the correlation functions measured by PCS in the time range $0.1\,\mu s - 10^3$ s.[4(c)] Moreover, the phenomenology of the main structural (α) process in strong glasses compared to that of the fragile counterparts is not yet established. The multirelaxational nature and the change of the α-relaxation time over a broad dynamic range, necessitates the use of many different spectroscopic techniques. Light scattering is a suitable tool for studying amorphous systems, due to its ability to probe both density and orientational fluctuations over a significant frequency range, however at low values of the wave vector q.

The objective of this paper is to present information on the dynamic and structural nature of both the primary and the

fast process of As_2O_3, a strong glass with directional bonds and covalent networklike structure, employing two dynamic light-scattering techniques, Brillouin scattering (BS), and photon correlation spectroscopy (PCS). In what follows we present a short background on dynamic light scattering (Sec. II A), and on the most important information related to the structure of As_2O_3 existing up to now (Sec. II B). Sections III and IV contain the experimental details and the way that data have been analyzed, correspondingly. The results and the discussion are presented in Sec. V in the spirit of recent models and phenomenologies concerning the glass transition problem. Finally, a summary is presented in Sec. VI, including the most significant conclusion that can be drawn from this study.

II. BACKGROUND

A. Dynamic light scattering

It is well established that light scattering is caused by spontaneous local variations in the dielectric constant.[6] These variations are the result of fluctuations in temperature, density, orientation of molecules, and concentration in the case of mixtures. Density and orientation fluctuations provide the dominant contribution to the scattered light in one-component systems. The choice of the proper scattering geometry enables one to measure the polarized (VV) or depolarized (VH) scattered intensity. The former is associated with the density and the later with the orientation fluctuations. Orientational or anisotropic contribution is also involved in the polarized part of the scattered intensity.

Two basic mechanisms are employed to account for the origin of the depolarized scattered light. One relates to the nonzero off-diagonal elements of the fluctuation polarizability tensor,[7] usually termed permanent optical anisotropy, whereas the other regards the dipole-induced dipole mechanism (second-order scattering) as the dominant contribution for the VH scattering.[8(a)] The former dominates when materials containing intrinsically highly anisotropic molecules are considered. A recent review of the difference in interpretation of depolarized light scattering and experimental considerations can be found in Ref. 8(b), where data from optically anisotropic molecular liquids are discussed.

The spectrum of the isotropic component consists of two central lines and the Brillouin doublet shifted symmetrically around the frequency of the incident light. One unshifted line (Rayleigh peak) due to entropy fluctuations is always present and usually accounts for a small fraction of the central peak. The second unshifted line (Mountain peak) due to structural relaxation (for viscoelastic fluids) can be resolved under certain conditions. The Brillouin doublet due to propagating pressure fluctuations is shifted to $\omega_B = \pm c_B q$ with $q = (4\pi n/\lambda_0)\sin(\theta/2)$ where c_B is the sound velocity, θ is the scattering angle, n is the refractive index of the medium, and λ_0 is the excitation light wavelength.

The propagation of density fluctuations is accompanied by dissipation in their energy content. Entropy fluctuations are diminished due to heat-diffusion processes, while pressure fluctuations or sound waves are mainly subjected to viscous dissipation. The inverse of the Brillouin peak linewidth (full width at half maximum), $\Gamma_B = a_B c_B/\pi$, is a measure of the phonon lifetime; a_B being the sound-attenuation coefficient. Temperature, as expected, plays a dominant role on the sound-wave characteristics; thus the increase of temperature results in a decrease in the hypersound velocity, due to a softening of the elastic constants of the medium and due to the dispersion. The sound attenuation passes through a maximum at $T_{\max}$, as the temperature evolves above T_g, and finally decreases to low values in the normal liquid state. The maximum in the attenuation coefficient at a given frequency ω_B, and the strong decrease in the speed of the sound signalize the onset of a *relaxation process*. Such a process occurs when energy is exchanged with a high rate τ^{-1} between structural units and propagative sound waves. Energy is transferred from the internal degrees of freedom to translational motion modifying the phonon characteristics. Therefore, an amount of information concerning details even on a molecular scale can be gained by measuring hypersonic properties of viscous liquids. The inverse of the Brillouin shift frequency at $T_{\max}$ is a good estimate for the structural relaxation time characterizing the process $\omega_B \tau \sim 1$.

Brillouin scattering has been extensively used to elucidate the dynamic behavior of organic materials.[7] In contrast, inorganic glass formers have received less attention by means of this technique. Inorganic materials studied include $3KNO_3$-$2Ca(NO_3)_2$ (CKN),[9,10] KCl-$2BiCl_3$,[11] SiO_2,[12] B_2O_3,[13,14] $ZnCl_2$,[15–17] $GeSBr_2$,[18] LiCl-$x H_2O$,[19] $x ZnCl_2$-$(1-x)ZnBr_2$ $(x=0, 0.25, 0.5, 0.75, 1)$,[20] $ZnCl_2$-MCl $(M=\text{Li, Cs})$,[20] $R Cl_3$-$AlCl_3$ $(R=\text{Gd, La})$.[21] Quitmann and coworkers were the first that compared their data with viscoelastic theory formulated in a Mori-Zwanzig ansatz.[17] By employing two relaxation channels they found no systematic deviations from the predictions in the whole interval $\omega\tau < 1, = 1, > 1$. They connected also the strength of the slow channel to the nonergodicity factor of the MCT in its primary version. In the case of $GeSBr_2$ they showed that stretching (nonexponential) effects can be also revealed by fitting the Rayleigh-Brillouin spectrum.[18] More recently, Cummins and co-workers have exploited the advantage of a tandem multipass interferometer to obtain high-resolution spectra.[8(a),22,23] The procedure they followed in analyzing their data is again a generalized hydrodynamic approach. In an attempt to predict the spectrum by using an approximate form of the MCT they found only qualitative agreement.[19] For long-wavelength density fluctuations the nonergodicity factor of MCT, and consequently the critical point T_c, could be determined by the limiting high- (Brillouin) and low- (ultrasonic) frequency sound velocities.[24] Further testing of this prediction,[22,23] has shown that the critical temperature can be reliably estimated by Brillouin scattering only if the memory function for the density fluctuations could be determined independently. The relaxation times obtained by the generalized hydrodynamics analysis suffer by a dramatic underestimation as the temperature is lowered to T_g. This finding indicates that fast relaxation should not be neglected in a memory function model.[8(a)] The shortcoming for such analyses that are able to predict line shapes is the fact that the models used are overparametrized; thus resulting to highly correlated values subjected to errors. From the experimental point of view the necessity of the generalized hydrodynamics becomes evident where the fit of three Lorentzians (Rayleigh plus Brillouin lines) fails.

From a different point of view, Kieffer and co-workers have used high-resolution Brillouin scattering to study network forming oxide glasses.[14,25–27] By probing structural changes in these systems, caused by either varying the temperature or by disrupting the structure adding alkali oxide modifiers, they were able to calculate the high-frequency complex mechanical moduli and thus to propose distinct mechanisms based on a molecular level to explain the structural relaxations in these systems.

In the high-frequency $\omega_B\tau \gg 1$ limit, which is satisfied at low temperatures near T_g, the Mountain (structural) relaxation is coupled to the nonoscillatory Rayleigh mode and can be best studied by photon correlation spectroscopy (PCS) over a broad time range (10^{-7}–10^{3} s). The strong temperature dependence of the relaxation time in this interval renders the dynamic behavior of the systems significant and necessitate the use of PCS which is capable to monitor the drastic temperature evolution of dynamic properties. Besides, the data obtained by PCS can be directly treated to give the width of the distribution for the relaxation times without being subjected to assumptions that could lead to misinterpretation of the data. This emerges from the rather simple three-parameter fitting used to the correlation function, as will be explained later. PCS probes both density and orientation fluctuations depending on the selected scattering geometry. The isotropic part of the correlation function is associated with entropy fluctuations that obey diffusive law and with the structural relaxation. On the other hand, the anisotropic part of the correlation function contains information concerning the orientational dynamics that arise mainly from fluctuations in the molecular optical anisotropy, as has been mentioned previously. Both reorientation and shear translational motion contribute to the depolarized dynamic light-scattering spectrum. The coupling between these two contributions renders the interpretation of the VH intensity quite complex. PCS has been mainly applied on amorphous polymers and molecular glass formers in order to investigate density, concentration, and orientation fluctuations. Only a few PCS studies in inorganic glasses [mixed alkali-silicate oxides,[28] zinc halides,[29] CKN,[30] B_2O_3 (Ref. 31)] have appeared in the literature so far. In particular, structural relaxation studies on strong glasses, which can be more easily found in inorganic than polymeric amorphous materials, are rare.[5]

B. Structural aspects of As_2O_3

Many experimental investigations have been devoted to the study of the different modifications of As_2O_3 during the last decades. The reason for this is provided by the structural peculiarities that this system exhibits.[32] In this part we shortly survey on the various structural studies of the amorphous state.

Arsenic trioxide exists in the solid state with three different crystalline modifications; the molecular arsenolite and the layered forms claudetite I and II, which bear a close resemblance. The melt-quenched glass is a stable colorless amorphous solid with a refractive index $n \approx 1.8$ and a glass transition temperature at $T_g = 160\,^{\circ}\mathrm{C}$.[33] It has been claimed that the very high viscosity far above the melting point indicates that the bonding of the atoms in the melt resembles that in claudetite.[32] Thus, rings with six and most probable with less and more members can be formed in the glass and maybe in the activated condensed phase.

Comparison of the x-ray-diffraction data between vitreous As_2O_3 and the two crystalline phases, arsenolite and claudetite, has revealed a close resemblance between the glass and claudetite I.[32] A reexamination of the glass structure with x rays having a better resolution led to the conclusion that the local structure, including two adjacent coordination polyhedra, can be better described by a new type of layer composed of three-membered rings of AsO_3 units.[34]

A complete vibrational study of all the different phases of As_2O_3 has long ago been performed.[35] It was suggested that glassy and liquid arsenic trioxide have both the same networklike structure where bridging oxygen atoms link pyramidal units.[35(a),35(b)] The pyramidal angle O-As-O was found larger than that in the crystals by an amount of about 20%. The data were interpreted in a way leading to the conclusion that the structure of the glass and that of claudetite bear a close resemblance. This speculation was further supported by an extended x-ray-absorption fine structure study, comparing data from the glass and the two crystalline phases.[36] No evidence for arsenolitelike entities was found in the glass,[36(a)] and furthermore, the interpyramidal As-O-As bond angle was concluded to remain unchanged in the glass as well as the crystal phases,[36(b)] in accordance with the findings of the Raman study.[35]

Additional analysis on the Raman spectra revealed the necessity for invoking both arsenolitelike and claudetitelike structures in order to account for the complete set of vibrational bands.[37] Along with the same lines was a computer relaxation analysis of a continuous random network model of glassy As_2O_3.[38] It was conjectured that the pyramidal angle O-As-O is not significantly different from that found in the crystalline modifications after a comparison of the experimental and the simulated radial distribution function with the second computed for both 98° and 114° O-As-O bond angles. Diffraction data employing neutrons were interpreted as a confirmation of the fact that claudetitelike regions do not have to be considered for a description of the glass structure.[39]

The above survey on the vitreous and liquid state of As_2O_3 made clear an existing ambiguity in the literature concerning the structural features of these states. Apart from an ultrasonic relaxation study at low temperatures deep in the glassy state there have been, to our knowledge, no other attempts to investigate the dynamic characteristics for this system.[40] The fact that an elucidation of the dynamic aspects of the glassy and the supercooled state are intimately associated with the structural ones, especially for network-type structures, has led us to perform a dynamic light-scattering experiment on arsenic trioxide—in the macroscopic as well as in the microscopic time domain—trying to shed more insight into the bimodal relaxation pattern that the system exhibits.[5]

III. EXPERIMENTAL DETAILS

A. Sample preparation

The purification procedure followed in order to obtain high-quality arsenic trioxide (Merck) have been described

previously.[35(b)] The optical cells, fused silica tubes with 10 mm o.d.–8 mm i.d., after carefully cleaning, were loaded with the chemical and were flame sealed under vacuum. The samples were kept at about 400 °C for several hours until the disappearance of the bubbles formed during the melting. A filtration process of the present system is impossible due to the extremely high viscosity of the melt even at temperatures far above the melting point.[41] However, high-purity samples were prepared by subliming the As_2O_3 directly into the optical cells.

B. Fabry-Perot interferometry

For the Brillouin-scattering experiment the monochromatic radiation was the $\lambda_0 = 488$-nm line emerging from an Ar^+-ion laser (Spectra Physics, 2040) operating in single mode with a stabilized power of about 200 mW. Measurements were performed at right-angle scattering in the polarized (VV) geometry. The incident beam was polarized by a Glan prism and the scattered light was analyzed by a Glan-Thompson prism (Halle, Berlin) with an extinction ratio better than 10^{-7}. The resolving element was a plane piezoelectricaly scanned Fabry-Perot interferometer (FPI) (Burleigh RC-110) used in a single pass arrangement. The interferometer had mirrors with flatness $\lambda/200$, 50 mm in diameter, reflectivity of about 0.98, and was driven by an external voltage produced by a ramp generator (Burleigh RC-43). A stabilization system (Burleigh Das-10) was controlling the FPI by locking the position of the Rayleigh and readjusting the mirrors parallelism in every scan maintaining thus the maximum finesse. The analyzed light was focused on a 200-μm pinhole and imaged onto the cathode of a cooled to -20 °C photomultiplier (Thorne-EMI) having a very low dark current. Photon counting electronics converted and transferred the signal to a computer where an acquisition interface board (Accuspec-CANBERRA) was recording the spectra with a scan rate 2 s. Measurements were completed when a satisfactory signal-to-noise ratio was reached, usually at 200 scans. The free spectral range was set at 25.56 GHz giving a good resolution of the Brillouin peaks in the whole temperature range. Despite of the fact that the contrast of a single pass interferometer is less than 10^3 and also that inorganic glasses exhibit usually too strong elastic scattering, in this work high resolution spectra were recorded with a finesse better that 75 reflecting the high purity of our samples and hence limited parasitic elastic light.

Polarized Rayleigh-Brillouin spectra of arsenic trioxide were recorded in the glassy, supercooled, and liquid state up to 500 °C. This upper limit of the investigated range is posed by a rapid increase of the vapor pressure of As_2O_3 as the temperature evolves, with the danger of explosion of the optical cell. Typical spectra are displayed in Fig. 1, representing the three different states of the system. Magnification factors for the Brillouin component are included reflecting the rather low value of the Landau-Placzek ratio, $I_R/2I_B$, with I_R and I_B being the integrated intensities of the Rayleigh and Brillouin lines, respectively.

C. Photon correlation spectroscopy

The correlation functions $G(t)$ of the polarized light-scattering intensity were measured at a scattering angle $\theta = 90°$ in the supercooled region 200–300 °C, e.g., in the temperature range where the α process was effectively into the time window of the technique. The light source was an argon-ion laser (Spectra Physics 2020) operating in single mode at 488 nm with a stabilized power of about 200 mW. The incident radiation was polarized vertically with respect to the scattering plane using a Glan polarizer. The scattered light was analyzed by a Glan-Thomson polarizer (Halle, Berlin) with an extinction coefficient better than 10^{-7}, allowing thus the detection of vertical (V) and horizontal (H) components and the measurement of the corresponding correlation functions $G_{VV}(t)$ and $G_{VH}(t)$.

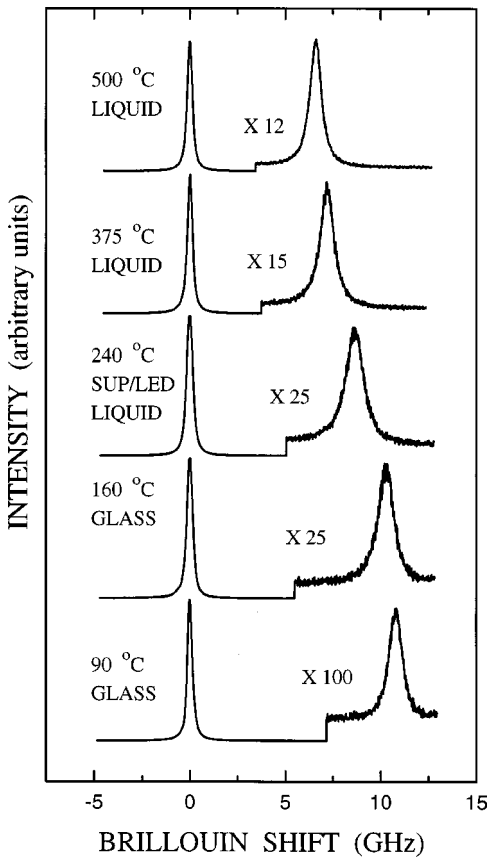

FIG. 1. Rayleigh-Brillouin spectra of glassy, supercooled, and liquid arsenic trioxide. The baselines are offset for better visibility. Magnification factors are also included reflecting the rather low value for the Landau-Placzek ratio as described in the text.

Polarized and depolarized (density and orientation) autocorrelation functions were measured on a broad time scale (almost nine decades, 10^{-6}–10^3 s) with a full multiple taut digital correlator (ALV-5000/FAST) with 280 channels. Arsenic trioxide used in this study seems to be dust-free and optically homogeneous displaying thus only intrinsic scattered light. Hence, under the assumption of homodyne conditions, the desired normalized electric field time-correlation function $g(t)$ is related to the recorded $G(t)$ by the relation,

$$G(t) = A[1 + f^* |\alpha g(t)|^2], \tag{3.1}$$

where A describes the long-delay-time behavior of $G(t)$ and f^* represents an instrumental factor obtained experimentally from measurements of the $G_{VV}(t)$ from dilute PS/CCl_4 solutions ($f^* = 0.5$). The parameter α is a measure of the fraction

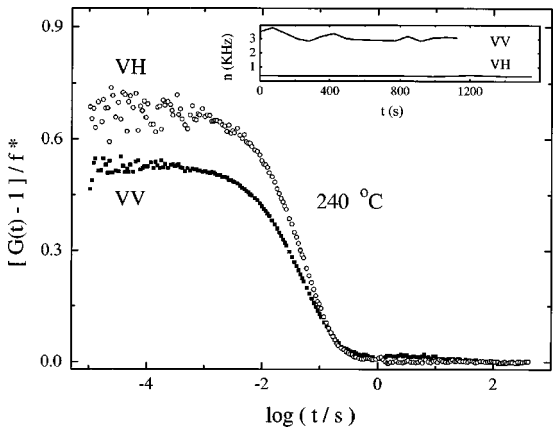

FIG. 2. Density and orientation autocorrelation functions for As_2O_3 at 240 °C Inset: Traces of the low total light-scattering intensity reflecting the homodyne conditions, (log denotes decimal logarithm).

of the total scattered light with correlation times longer than about 10^{-6} s. Figure 2 shows polarized and depolarized intensity net correlation functions $[G(t)/A-1]/f^*$ at 240 °C.

IV. DATA ANALYSIS

A. Rayleigh-Brillouin spectroscopy

Polarized Brillouin spectra provide the dynamic structure factor $S(q,\omega)$ at low wave numbers. The form of $S(q,\omega)$ for such long-wavelength density fluctuations has been theoretically predicted for systems composed from molecules with internal degrees of freedom.[42] If the thermal diffusivity mode (Rayleigh line) is not taken into account then the dynamic structure factor can be cast in the form

$$S(q,\omega)=\frac{2v_0q^2}{\omega^2}\,\mathrm{Im}[\omega^2-q^2c_0^2-i\omega q^2\Phi_L(q,\omega)]^{-1}, \tag{4.1}$$

where v_0 is the thermal velocity, c_0 is the adiabatic sound velocity, and $\Phi_L(q,\omega)$ is the Fourier transform of the $\Phi_L(q,t)$, the memory function for the longitudinal kinematic viscosity. Until $\Phi_L(q,\omega)$ is specified explicitly no approximation is being involved. Thus, the specific features of the problem under study should be incorporated in the modelization of the memory function. Various models have been so far utilized for $\Phi_L(q\omega)$, including single exponential relaxation, stretching effects, empirical forms, slow and fast processes.

In our case we have to model $\Phi_L(q\omega)$ so as to account for both the fast and slow process. Such a phenomenological ansatz has been previously made by using a weighted sum of two terms representing α and β relaxation in analyzing Brillouin data for an organic glass former.[43] However, in the case of As_2O_3 the contribution of the slow process has a negligible effect on the Brillouin linewidth for the whole temperature range studied, since the PCS data indicate that structural relaxation is effectively frozen at such temperatures.[5] Following the procedure of Ref. 43 the memory function for the longitudinal kinematic viscosity can be written as

$$\Phi_L(q\omega)=(c_\infty^2-c_0^2)q^2[\tilde{f}\Phi_\alpha(\omega)+(1-\tilde{f})\Phi_\beta(\omega)], \tag{4.2}$$

with Φ_α and Φ_β being, respectively, the parts of the memory function describing the slow (α) and the fast (β) processes, which are considered as Debye-like ones:

$$\Phi_i=\frac{1}{\omega}\left[\frac{i\omega\tau_i}{1-i\omega\tau_i}\right], \quad i=\alpha,\beta, \tag{4.3}$$

$\tilde{f}$ is a parameter accounting for the relative weight of the two processes. In this sense, $\tilde{f}$ can be related to the magnitude of the longitudinal modulus that is relaxed by the slow process,

$$\tilde{f}=\frac{c_{\alpha\infty}^2-c_0^2}{c_\infty^2-c_0^2}. \tag{4.4}$$

With this imposition, an additional sound velocity $c_{\alpha\infty}$ has been introduced that can be obtained when the relaxation rate of the slow (fast) process is much shorter (longer) than the frequency, or $\omega\tau_\alpha\gg1$ and $\omega\tau_\beta\ll1$.

Under the above considerations the memory function will read

$$\Phi_L(\omega)=\Phi_0+\frac{c_{\alpha\infty}^2-c_0^2}{i\omega}+i\,\frac{c_\infty^2-c_{\alpha\infty}^2}{\omega}\left(\frac{\tau_\beta}{1+i\omega\tau_\beta}\right), \tag{4.5}$$

where the first term Φ_0 represents a background Brillouin linewidth. Substituting Eq. (4.5) in Eq. (4.1) there remains an expression including the quantities $\Phi_0, c_{\alpha\infty}, c_\infty, \tau_\beta$, which in the subsequent analysis are treated as free-fitting parameters.

B. Photon correlation spectroscopy

The information obtained by light scattering from an isotropic medium depends on the polarization of the incident in respect the scattered light.[6(a)] Fluctuations in dielectric constant $\delta\varepsilon_{zz}(q,t)$ determine the electric-field correlation function $C_{\mathrm{VV}}(q,t)$ of the polarized scattered light. In a single-component system $\delta\varepsilon_{zz}(q,t)$ is proportional to the qth component of the number density fluctuations $\delta\rho(q,t)=\Sigma_j\exp[iqr_j(t)]$, with $r_j(t)$ being the position of the jth molecule,

$$C_{\mathrm{VV}}(q,t)=\left(\frac{\partial\varepsilon}{\partial\rho}\right)^2\langle\delta\rho(q,t)\,\delta\rho(q,0)\rangle/\langle|\delta\rho(q,0)|^2\rangle. \tag{4.6}$$

In the depolarized geometry, scattered light is determined by the fluctuations in $\delta\varepsilon_{yz}(q,t)$ that arises from the fluctuations $\delta\alpha_{yz}(q,t)=\Sigma_j\alpha_{yz}^j(t)\exp[iqr_j(t)]$ in the molecular optical anisotropy $\alpha_{yz}(q,t)$, where α_{yz}^j is the yz component of the jth molecule. Then the corresponding normalized correlation function reads

$$C_{\mathrm{VH}}(q,t)=\langle\delta\alpha_{yz}(q,t)\,\delta\alpha_{yz}(q,0)\rangle/\langle|\delta a_{yz}(q,0)|^2\rangle. \tag{4.7}$$

As can be seen from Fig. 3, the experimental time correlation functions, found to be q independent in the time domain studied, present only one decay in both scattering ge-

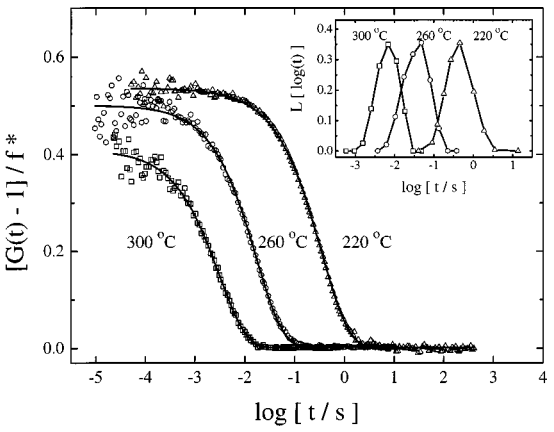

FIG. 3. Depolarized intensity correlation functions fitted with the KWW function [Eq. (4.8)] for three different temperatures. Inset: Distribution of the relaxation times obtained by inverse Laplace transform (ILT) analysis [Eq. (4.9)].

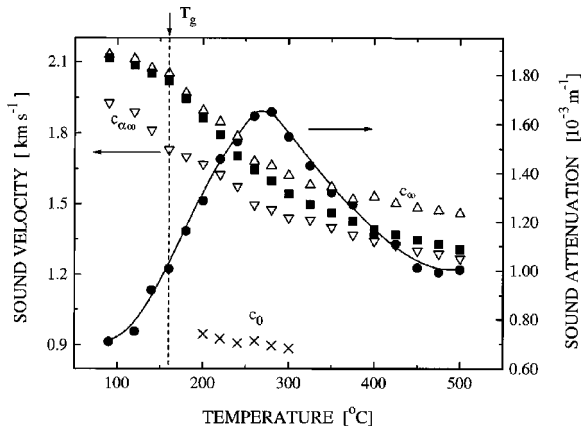

FIG. 4. Temperature dependence of the viscoelastic parameters of As_2O_3. Solid symbols: data from DHO analysis, c_B (squares), Γ_B (circles). Open symbols: parameters from fitting with the phenomenological memory function [Eq. (4.1)], c_∞ (up triangles), $c_{\alpha\infty}$ (down triangles), c_0 (crosses).

ometries, namely the α process. Structural relaxation is frequently described by the stretched exponential or Kohlrausch-Williams-Watts (KWW) equation that is used as a two parameter, τ^*, β_K, fitting function,

$$g(t) = \exp[-(t/\tau^*)^{\beta_K}]. \tag{4.8}$$

The exponent β_K, usually called the shape parameter, is a measure of the departure from the single exponential or Debye relaxation and seems to exhibit a correlation with the non-Arrhenius character of the α process.[44] There is still no consensus on the microscopic origin of Eq. (4.8), e.g., if it emerges from heterogeneous (single exponential with different relaxing time scales) or homogeneous (intrinsic nonexponential decay) relaxation.[45]

Approaching $g(t)$ in a different way, the inverse Laplace transform (ILT) analysis can be used. This procedure employs a superposition of single exponential functions emerging from different spatial relaxing domains in the system, being thus compatible with the heterogeneous scenario mentioned above. Therefore, the field correlation function is the weighted sum of these individual contributions

$$g(t) = \int L(\log\tau)\exp(-t/\tau)d\log\tau, \tag{4.9}$$

where $L(\log\tau)$ reflects the distribution of the relaxation times and is directly provided by Laplace inverting the above relation. The advantage following this approach is that no assumptions are made on any particular form of $L(\log\tau)$.

V. RESULTS AND DISCUSSION

A. Brillouin scattering—fast process

Figure 4 displays the temperature dependence of the sound-velocity (solid squares) and the sound-absorption coefficient (solid circles), obtained from the Brillouin peak position and width after fitting the spectra with the damped harmonic oscillator (DHO) ansatz, i.e., Lorentzian line shapes. $S(q,\omega)$ reduces to the DHO form when the fast relaxation term in Eq. (4.5) is neglected. The value $n=1.8$ was used for the refractive index and was assumed constant for the temperature range studied, as usually occurs for the most oxide glass-forming liquids.[33] The main unexpected features revealed from the temperature dependence for the quantities c_B and α_B have been described in detail,[5] and can be briefly summarized as follows. (i) Strong relaxation takes place in the sub-T_g region, reflected both in the sound-velocity rapid drop and more clearly in the rather large value of the absorption coefficient (almost 50% of its maximum value), near T_g. (ii) The phonon energy dissipation maximum $T_{\max}$ occurs at much lower temperature than the normally expected. Being more specific, as we have discussed,[5] the $T_{\max}-T_g$ difference furnishes an insight of the fragile character of the supercooled liquid.[46] In the case of As_2O_3 a very large difference should be expected that, in fact, is not observed. Furthermore, a second peak in the $\alpha_B(T)$ curve is probably hidden at high temperatures, whose beginning is reflected in the change of the slope of $\alpha_B(T)$ around 500 °C.

From the above arguments it becomes evident that the relaxation process revealed by BS in the vicinity of T_g owns

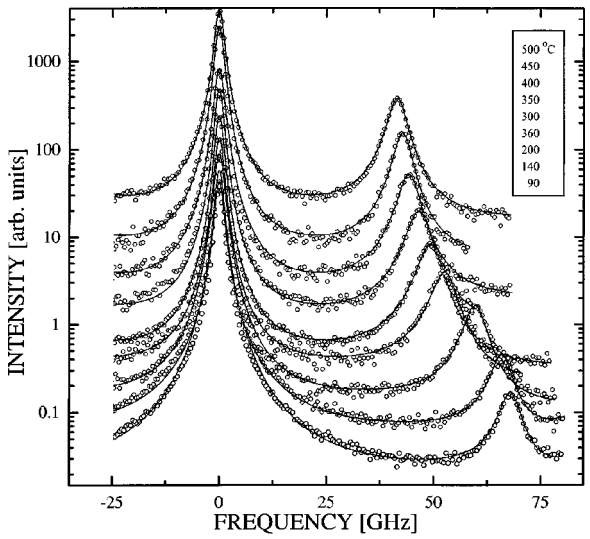

FIG. 5. Rayleigh-Brillouin spectra of As_2O_3 at the indicated temperatures (open points) and best fits with Eqs. (4.1)–(4.5), (solid lines). Only 20% of the data points are plotted for better clarity.

the features of a fast (secondary) β relaxation definitely distinct from the slow (primary) α relaxation. It is tempting, thus, to try to unravel the subtle characteristics of this process by using the ansatz of Eq. (4.1)–(4.5) to fit the experimental data. The best curves are presented as solid lines in Fig. 5 displaying a satisfactory agreement between the experimental data and the used model. The parameters of the model were obtained from least-squares fits taking into account the broadening due to the instrumental response by convoluting each spectrum with the apparatus resolution function. In Fig. 4 the viscoelastic parameters are presented together with the c_B and α_B values obtained from the position and the width of the Brillouin peaks. The constant term in the memory function, Φ_0 in Eq. (4.5), appears eventually as temperature independent with a value close to 1×10^9 rad s^{-1}.

As expected, the high-frequency-sound velocity c_∞ almost coincides with the experimentally measured c_B at temperatures close to T_g. For higher temperatures the dependence of c_∞ seems to deviate from a linear form, as usually happens when treated as a free-fitting parameter. The alternative choice is to force fit the spectra with a linear decreasing c_∞ that vanishes at the same temperature with c_0.[43] On the other hand, $c_{\alpha\infty}$, the high-frequency sound velocity that characterizes the low-temperature response of the pure α process, is found smaller than the measured values of c_B indicating that a portion of the relaxed modulus is due to the fast β process. Similar behavior was found for the fast process for (*o*-terphenyl) glass,[47] but the closeness of the fast and slow process (small temperature difference) made it impossible to elucidate the features of the fast one for a broader temperature scale. On the contrary, the large separation of the two processes in As_2O_3 enables the estimation of the characteristics of the fast β process in the whole temperature range, for the first time. The close proximity of $c_{\alpha\infty}$ and c_B at high temperatures, where the fast β process has already relaxed, is also an indication of the correct physical meaning of the extracted parameters. This further suggests that $c_{\alpha\infty}$ will evolve as the continuation of c_B, when the α process becomes active for the Brillouin frequency window, i.e., at $T>500\,^\circ$C.

Under the guidelines of the model used, the low-frequency sound velocity c_0 does not enter in the fitting procedure. However, a rough estimation of its magnitude can be obtained as follows. According to Eq. (4.4), the parameter $\tilde{f}$ is defined as the relative weight of the two processes reflecting the amount of the longitudinal modulus relaxed by the slowest one. This contribution can be independently concluded through the density autocorrelation functions. Specifically, the ''contrast'' of $g(t)$, α, is indicative of the scattered intensity with dynamics slower than 10^{-6} s; thus the following approximation may hold, $\alpha\approx\tilde{f}$. Within the temperature range of PCS $\tilde{f}$ assumes the value of 0.7; then Eq. (4.4) yields for c_0 the values plotted in Fig. 4. It can be discerned from the magnitude and the temperature dependence of c_0 that it would assume values comparable with these of c_B when the α process will be relaxed. This is expected to occur at a temperature $T\approx4T_g$ (see Fig. 9 below).

A significant outcome of the fit is the relaxation time of the fast process and its temperature dependence as well. In

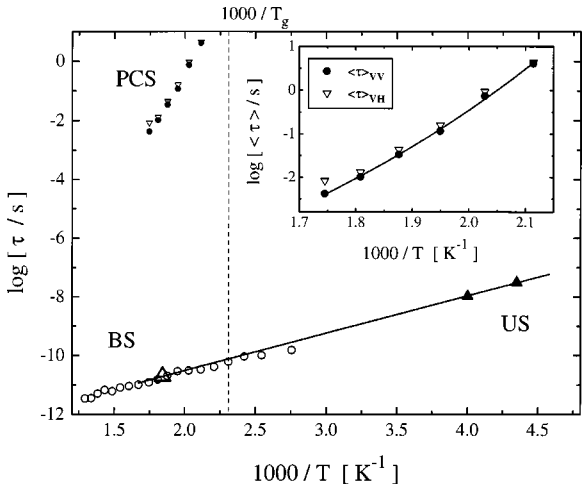

FIG. 6. Temperature dependence of the mean relaxation time. The BS and PCS data reveal the large gap in the dynamics of As_2O_3 at the same temperature. The ultrasonic (solid triangles) and the BS relaxation times from $T_{\max}$ (open up triangle) seem to conform nicely to an Arrhenius temperature with very low activation energy. The same temperature dependence is obeyed from the relaxation times obtained from fits to individual spectra (open circles). In the inset we have magnified the PCS region. The vertical dashed line indicates T_g.

Fig. 6 the relaxation times are reported (open circles) for the temperature range of the Brillouin-scattering measurements. The data are found to follow an Arrhenius law with low activation energy, as expected for fast relaxations. The activation energy of this fast process (E/k_B) results to about 2700 K, while values of about 800 K are reported for the fast process when fragile systems are considered.[47] This difference could be understood on the basis of the contrasted nature of fast relaxations in strong and fragile liquids, as discussed below. A rough estimate for the activation energy for this process is also obtained from the frequency dependence of the $T_{\max}$. The absorption maximum at hypersonic frequencies yields for the relaxation time $\tau_{\max}\approx1.91\times10^{-11}$ s at 270 °C. The ultrasonic loss measurements, far below T_g, for As_2O_3 provide two more values for the relaxation time.[40] These values result in an activation energy comparable with the one mentioned above. This temperature dependence is plotted as a solid line in Fig. 6.

The issue of different activation energies for the fast relaxation times may be related to the mechanism generating fast-localized motions, which in turn become evident as fast relaxations. The basic idea is the existence of two-level systems in a glass where the energy of each system is described by an asymmetric double-well potential,[48] in which the asymmetry and the height barrier between the two wells depend on neighboring local structure. Some external parameters govern the population of the two levels and the transition between the two minima is the reason for the onset of a relaxational process. This concept applies for both strong and fragile systems; the essential difference between them has to be sought in the way that temperature affects the neighboring environment of the relaxator and hence the potential well stability. Being more specific, in strong glasses the shape of an asymmetric double-well potential is expected to change less when temperature alters, compared with the correspond-

ing in fragile systems. As a result, thermal activation in fragile structures is facilitated also by changes in the features of the potential well. On the contrary, in strong glasses, the local environment of a relaxing unit preserves the stability of the potential well rendering the intrawell relaxation time a well-defined quantity. In other words, the relation of the characteristic time for the relaxing unit τ_β compared to the fluctuation rate of the well itself, ω_w^{-1}, may have a strong impact of the observed difference in activation energies. The ''adiabatic'' limit $\tau_\beta \ll \omega_w^{-1}$ corresponds to strong—while the opposite limit, $\tau_\beta \gg \omega_w^{-1}$, to fragile—glasses. A qualitatively different relaxation pattern in the fast dynamics regime was recently found in computer simulations when the microscopic dynamics was altered exhibiting Newtonian or Brownian behavior.[49] More specifically, Newtonian dynamics results in abrupt fast β decay separated from the slower one by a well-defined plateau, while in the stochastic dynamics (Brownian) approach the decay is much more gentle. From the experimental point of view it is obvious that interactions in strong glasses are mainly of deterministic character (Newtonian) while in fragile ones stochastic dynamics prevail.

Another interesting feature of the examined system, that deserves to be addressed, is the strong sound-velocity variation (almost 60%) near T_g, and the persistence of relaxation even in the sub-T_g region. This observation combined with the fact that the boson peak of As_2O_3 experiences a vibrational softening,[50] stands at the basis of the vibration-relaxation model that attributes a vibrational origin to the fast process.[51] This arises from the notion that fast relaxations appearing deep in the glassy state cannot be assigned to flow processes but they are rather related to anharmonic double-well potentials.

In Ref. 5 we commented on the necessity for employing a structure-specific mechanism in order to account for this fast mode that was found in the strongly correlated supercooled state for As_2O_3. This mechanism was further generalized and found to be compatible with our low-frequency Raman data for this system.[50] In the framework of this structural mechanism in an oxide glass there can be a variety of different local environments conserving, to some extent, the local structure of the different crystalline phases that the material possesses. These states correspond to the various local minima of the free-energy curve where their energy difference and the barrier height between them depends on the neighboring environment. Thus, a propagating phonon can be resonantly absorbed by the two-level systems resulting to the observed dissipation. This attempt at utilizing fast relaxations through two-level systems is one of the few that employees a certain molecular entity processing two metastable configurations; where the interplay between these corresponds to the hopping over the potential barrier.[40,52]

It should be noted here that two kinds of structural changes have been obtained by molecular-dynamics simulations in B_2O_3.[53] In the process taking place below 1500 K the 67% of B atoms that were initially twofold coordinated are gradually decreased upon cooling by transforming to threefold coordinated. In the second structural change below 1000 K part of the threefold-coordinated B atoms are further increasing their bonding rendering the structure a mixture of both three- and four-coordinated B atoms. The second process follows qualitatively the idea that we have developed in Ref. 50 in order to account for the fast relaxations observed in strong oxide glasses. The significant factor seems to be the existence into the amorphous phase of microdomains, which facilitate the formation (in a distorted way) of the different crystalline structures that the material possess. Dynamic heterogeneity arises naturally from these considerations. On the other hand, the process involving the disruption of the structural unit itself is reminiscent of the continuation of the primary or α relaxation in the liquid state.

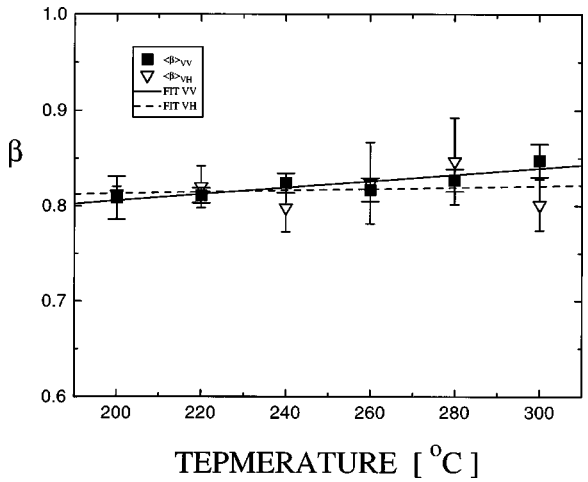

FIG. 7. Stretching exponent as a function of temperature for density and orientation scattering geometries. Solid and dashed lines denote linear temperature dependence.

Before closing this section it should be useful to try to check in some way the validity of the structural mechanism envisioned in Ref. 5, to explain the nature of the fast process. If the proposed scheme is intuitively correct, then it is expected that the $c_B(T)$ curve should be restricted between the limits posed by the sound velocities of the two crystalline polymorphs, claudetite I and II. A rough estimate of the mean-velocity ratio for these crystals, $R=\langle c_{\rm I}\rangle/\langle c_{\rm II}\rangle$, where $\langle c_i\rangle$, i=I,II denotes the product of the longitudinal and the two transverse velocities, can be made by the following equation $\varepsilon = k_B T[\ln\langle c_{\rm I}\rangle/\ln\langle c_{\rm II}\rangle]$.[54] Using the above equation and data from Ref. 32 we find $R\approx 1.55$. Furthermore, we see from Fig. 4 that the ratio of the low-T (glass, $c_g \leftrightarrow c_{\rm I}$) to the high-$T$ (liquid, $c_l \leftrightarrow c_{\rm II}$) velocities is of the same magnitude with R, $c_g/c_l \approx 1.6$, supporting the idea of the pseudotransformation occurring in the supercooled liquid.

B. Photon correlation spectroscopy—*a*-relaxation

The KWW or stretched exponential function [Eq. (4.8)] was used to model the electric field time correlation function $g(t)$. This three-parameter equation is found to fit adequately the experimental data for As_2O_3 as shown in Fig. 3 for three different temperatures in the supercooled state. The solid lines represent the KWW function that was found to assume for the shape parameter virtually the same mean value $\langle\beta_K\rangle = 0.82 \pm 0.02$ for both density and orientation fluctuations, characterizing this system as one of the strongest glass-forming liquids in Angell's classification.[55] The temperature dependence of $\langle\beta_K\rangle$ is shown in Fig. 7, and the corresponding ILT analysis of these time correlation func-

tions is presented as an inset. The apparent similarity between the different distributions of the relaxation times and the lack of any bimodal pattern in the ILT peaks is in accord with the KWW fitting procedure.

Adopting the idea that the shape parameter β_K is an indication of the cooperative dynamics and noting that it has the same magnitude for both scattering geometries, it can be concluded that density and orientation fluctuations are strongly correlated exhibiting the same degree of cooperativity. This is, to some extent, expectable for networklike structures where the covalent bond is the dominant feature. Indeed, the microscopic origin of relaxation processes can only be understood by considering the specific features of the system under study. Considerable importance should be paid to the geometrical characteristics of the relaxing unit and the nature of the chemical bonding between them. For systems with simple molecules frequently exhibiting fragile behavior, rattling of particles in transient cages formed by their relatively large number of neighbors (10–14) is employed as a general picture of the fast relaxation mechanism. On the contrary, for the relatively low coordination number (3–4) systems interacting with strong directional covalent bonds, the aforementioned mechanism (caging) ceases to capture a physical meaning. Consequently, certain structural changes compatible with the ingredient of stable structural units should be sought as possible mechanisms for relaxations. Among them can be envisaged movements such as: (i) small fluctuations in the positions of the atoms (limited by their localization length), (ii) small distortions of the angles bridging structural units. Of course, it is easily conceived that these two kinds of motions closely associated with density and orientation fluctuations are highly correlated in network glasses. This correlation arises from the fact that translational movements of a structural unit with strongly attached vertices involve also a small reorientation of its bonds.

The relaxation time obtained from the KWW analysis exhibits strong temperature dependence as is normally expected in the supercooled state. The temperature dependence of the relaxation time for both density and orientation correlation functions is plotted in Fig. 6. The values resulted from the fitting have been transformed to the mean relaxation time through the relation

$$\langle \tau \rangle = \tau^* \beta_K^{-1} \Gamma(\beta_K^{-1}), \tag{5.1}$$

where $\Gamma(x)$ is the gamma function. If the mean relaxation time is force-fitted to obey an Arrhenius temperature dependence near T_g, $\langle \tau \rangle = \tau_0 \exp(T_\alpha/T)$, then the effective activation energy T_α ($T_\alpha = E_{\rm eff}/k_B$), and the microscopic relaxation time can be estimated $T_\alpha = 1.9\times 10^4$ K (37.4 kcal mol^{-1}) and $\tau_0 = 1.67\times 10^{-17}$ s. The limiting high-temperature value τ_0 is too short implying thus possible deviations from the Arrhenius form. Using the above values, T_g can be estimated as the temperature where the relaxation time $\tau(T_g) \approx 10^2$ s, this results in $T_g \approx 163\,^\circ$C, which is in excellent agreement with the experimental value.

Alternatively, the temperature dependence of the mean relaxation time can be described by a generalized Arrhenius relation[55]

$$\langle \tau \rangle \sim \exp\left[\frac{DT_0}{(T-T_0)^n}\right], \tag{5.2}$$

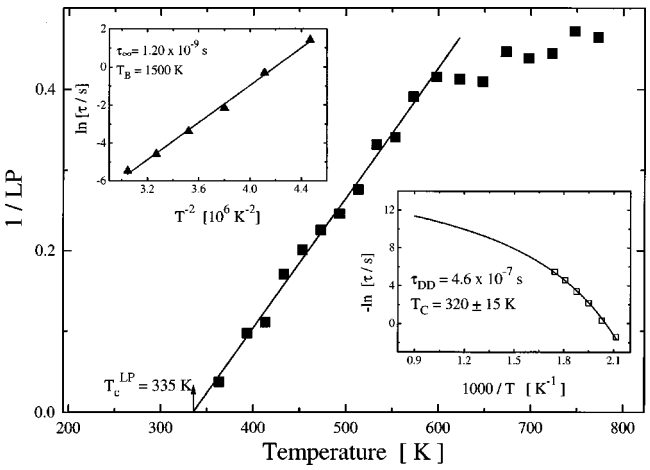

FIG. 8. Temperature dependence of the inverse of the Landau-Placzek ratio in a range including glass, supercooled liquid, and the melt. The straight line is the prediction of the two-fluid model of Ref. 2(d). Inset: VFT prediction of the same model and the specific temperature dependence of Bässler model valid at low temperatures, (ln denotes natural logarithm).

where the strength index D, the ideal glass transition T_0, and the exponent n are temperature-independent quantities. The value $n=1$ leads to the simple Vogel-Fulcher-Tammann (VFT) expression with T_0 usually identified with the Kauzmann temperature,[55] lying below T_g, and consequently being dynamically inaccessible. A value $n=\frac{3}{2}$ emerges from a two-fluid picture for a system near the glass-liquid transition.[56]

From a modified Arrhenius plot, the fragility m of a system can be determined as the slope of the mean relaxation time at the lowest-temperature interval given by the expression

$$m = \left.\frac{d \log_{10}\langle \tau \rangle}{d(T_g/T)}\right|_{T=T_g}. \tag{5.3}$$

The fragility index can be also calculated by the equivalent expression $m = \log(\tau_0^{-1}) + \log \tau(T_g)$,[55] where τ_0 is the preexponential factor in a forced Arrhenius fitting. By using the value found previously for τ_0, the above equation yields for the fragility index $m \approx 20$ (experimental value $m \approx 19$) implying that As_2O_3 is one of the strongest liquids as SiO_2 and GeO_2.[44] The strength index D is related to the fragility parameter m via the expression $m = 16 + 590/D$, yielding the value $D \approx 200$. With D fixed, the ideal glass transition temperature for As_2O_3 can be estimated to be $T_0 \approx 70$ K. This value is, as expected, very low compared with T_g; the reason is that strong liquids exhibit their dynamic singularity at a ratio T_0/T_g, much lower than fragile ones.

Bimodal patterns of relaxation, apart from MCT and the coupling model, are also predicted by two-fluid models.[2(d)] The picture emerging from such models is a liquid structure consisting of an isotropic fluid phase concentrated by denser regions that are dominated by long-lived order parameter fluctuations (OPF), defining the defect-rich phase. OPF are attributed to spatial fluctuations of finite wavelength and lifetime. Temperature decrease results to defect clustering below the melting point, and the reduced defect mobility as the

temperature is further lowered leads to a percolation of the defect regions at a point identified with T_g. The two-fluid model[57] aims to rationalize the VFT relation, the Kauzmann paradox,[56] and the recently observed ultraslow mode and the excess light-scattering intensity.[57(a)] The latter is produced by concentration fluctuations of the defects, that modulate the refractive index of the medium, and becomes evident through the Landau-Placzek (LP) ratio increase, when lowering temperature. Simple thermodynamic fluctuation theory arguments have led to the result that the inverse of the LP ratio should follow a linear T dependence, for low temperatures, as indeed is shown in Fig. 8. The intercept,[58] $T_C^{\mathrm{LP}} \approx 335\,\mathrm{K}$, of 1/LP with the T axis designates the temperature at which defect fluctuations would lead to infinite excess light-scattering due to the concomitant phase separation of the liquid to defect-free and defect-rich phases. However, this expected phase separation is avoided because the thermodynamically allowed OPF are kinetically prohibited at such low temperatures. The critical point T_c can be further estimated by a VFT-type law predicted by the model.[2(d)] Such a plot is seen in the lower inset of Fig. 8, where the obtained dynamic criticality is estimated to be at $T_c \approx 320\,\mathrm{K}$, very close to the value obtained from the LP ratio temperature dependence; although higher enough from the T_0 provided from the modified VFT relation. It should be mentioned here that the spectra at such temperatures do not, of course, exhibit infinite elastic scattering. It may be also important the observation of the slope change in the 1/LP vs T curve at a temperature close to the $T_{\max}$, signalizing probably the onset of the defect-rich phase formation.

More recently, Vilgis has reported on a simple phenomenological approach, to account for many experimental facts related to the glass transition problem;[59] this is based solely on the energetic and structural randomness found in supercooled liquids. The key feature of the model is the fluctuation of the coordination number, Δz, around the mean value z_0. This parameter Δz can be used to discriminate between simple liquids and network structures. The confinement of the atoms in the later case yields vanishingly small values for the fluctuation Δz, while finite differences in the coordination number are found in simple liquids. The strength index D is related to Δz through $D=\frac{1}{4}(z_0/\Delta z)^2$. This condition naturally accounts for the strong-fragile classification, resulting in $\Delta z \approx 0.1$ for As_2O_3 ($z_0=2.4$). This is an acceptable value for the fluctuation of the coordination number in strong liquids, supported also by the neutron-diffraction results,[39] while values as large as 3 or 4 occur in simple liquids.[60]

It was also shown[59] that in the limit $\Delta z \to 0$ the VFT equation assumes a form, being valid at low temperatures, as proposed by Bässler,[61] starting from a different point of view (see upper inset in Fig. 8). Bässler's temperature T_B relates to z_0 and E_0 parameters in Vilgis' model via $T_B = z_0 E_0/2^{1/2}$. Thus, for As_2O_3, it is roughly estimated the variance $E_0 \approx 850\,\mathrm{K}$ ($1.7\ \mathrm{kcal\,mol^{-1}}$) for the energy fluctuations in the random-phase energy landscape characterizing this system. Beyond the strong-fragile discrimination, the most important prediction of the mentioned approach concerns the correlation between the Kohlrausch exponent β_K with other parameters, $\beta_K \approx 1-\Delta z E_0/T$, as well as the correlation of β_K with fragility $D=(T_0/T_g)^2/[1-\beta_K(T_g)]^2$. A calculation of β_K at $T=573\,\mathrm{K}$ yields the value $\beta_K \approx 0.77$ in relatively good agreement with the experimental value; although the strength index is underestimated when obtained by the previous equation. Finally, it is worth mentioning a close dynamic similarity between the arsenic trioxide studied here and two polymers; poly(*n*-hexylmethacrylate),[62(a)] and poly(*n*-lauryl methacrylate),[62(b)] where in both cases slow and fast processes were found near T_g.

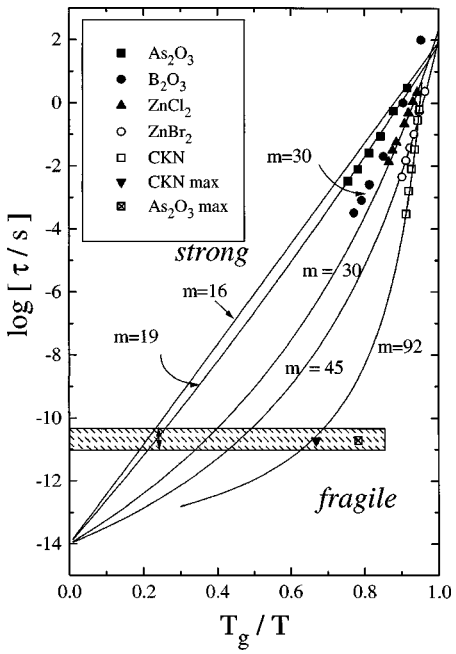

FIG. 9. Fragility plot for a class of inorganic liquids. As_2O_3, our data; B_2O_3, data from Ref. 4(a); $ZnCl_2$ and $ZnBr_2$, data from Ref. 29; CKN $\{2\,Ca(NO_3)_2\,3\,KNO_3\}$, data from Ref. 30(a).

VI. CONCLUDING REMARKS

In this work we have dealt with the dynamic study of the glass transition and the accompanying phenomena in a strong inorganic glass former. Fragility, cooperativity, dynamic heterogeneity, non-Debye behavior, and two-step relaxation processes are the most important discussed issues of glass transition. As a consequence, an understanding of the molecular origin of the dynamical features of supercooled liquids is essential in the explanation of the mentioned concepts.

Fragility, an empirically introduced material property, reflects the ease of structure change under temperature variations, and naturally relates to the kind of intermolecular interaction. The density of minima of the energy surface in configuration space can be translated to the degree of fluctuation of the coordination number.[59] From this point of view, As_2O_3 appears to be one of the strongest liquids with $m \approx 19$. The well-defined short-range order in such kind of covalently bonded materials enables the existence of order up to a medium range. Consequently, quasiordered structures, modestly affected by temperature changes appear less fragile. A comparison of the different degree of the fragility exhibited by some inorganic liquids can be seen in Fig. 9. The shaded region denotes the location of the α-relaxation times, in the time region of the Brillouin spectroscopy, and the expected value for As_2O_3 is marked by the double arrow

at $T \approx 4T_g$. However, for As_2O_3, the measured relaxation time is indicated by the crossed square.

Cooperativity, in its general sense, becomes important when cooling imposes sluggish behavior on the molecules rearrangements and their diffusion. The spatial coordinated motion defines the cooperativity length.[63] This concept is a genuine *dynamic* feature and consequently cannot be seen in the static structure factor as in the case of a *static* correlation length. Dynamic heterogeneity can be generally expressed as the presence in the liquid of a diverse set of spatial regions. The diversity stands on the basis that molecular properties are differentiated at such regions. This idea has been considered as a possible candidate responsible for the onset of stretching and is supported experimentally by multidimensional NMR studies.[64] The stretching effect in As_2O_3 is almost negligible. The narrow distribution of relaxation times follows probably from the inability for structural changes to occur on a short range. Under these conditions relaxation should take place through strains relief of the three-dimensional network at an intermediate spatial range, preserving the coordination polyhedra almost unperturbed. Thus, proceeding via certain channels, relaxation is plausibly anticipated to be a topological property of the space in which the relaxator is embedded.[65]

The two-step decay relaxation scenario still remains one of the puzzling features in viscous liquid dynamics. Fast processes, in the picosecond time domain, are predicted as the early stages of relaxation by recently developed theories and phenomenological models. Their time dependence cannot be undoubtedly answered with the available experimental data. In As_2O_3 a fast process revealed by the Brillouin-scattering technique, has been assigned to conformational transitions between specific liquid structures. These structural changes are not expected to contribute to the network degradation at such temperatures in contrast to the assignment of the low-temperature process observed in B_2O_3.[14] It has indeed been shown for B_2O_3 by using NMR spectroscopy,[66] that its network remains almost unchanged up to very high temperatures.

[1] (a) See, *The Proceedings of the Second Workshop on Non-Equilibrium Phenomena in Supercooled Fluids, Glasses and Amorphous Materials*, Pisa, Italy [J. Phys.: Condens. Matter **11, (10A)** (1999)]; (b) see, *The Proceedings of the Third International Discussion Meeting on Relaxations in Complex Systems*, edited by K. L. Ngai, E. Riande, and M. D. Ingram, J. Non-Cryst. Solids, **235-237** (1998); (c) see, the collection of papers in *Supercooled Liquids: Advances And Novel Applications*, edited by J. Fourkas, D. Kivelson, U. Mohanty, and K. Nelson, ACS Symposium No. 676 (American Chemical Society, Washington, D.C., 1997); (d) see, the collection of papers in Science **267**, 1924 (1995).

[2] (a) For a review on the theory, see, W. Götze and L. Sjögren, Rep. Prog. Phys. **55**, 241 (1992); for a review on recent tests of the MCT, see W. Götze, in *Proceedings of the Second Workshop on Non-Equilibrium Phenomena in Supercooled Fluids, Glasses and Amorphous Materials, Pisa, Italy* [Ref. 1(a)], pp. 1–45; (b) K. L. Ngai and R. W. Rendell, in *Supercooled Liquids: Advances and Novel Applications* [Ref. 1(c)], pp. 45–66; (c) S. Kivelson, X. Zhao, D. Kivelson, T. M. Fischer, and C. M. Knobler, J. Chem. Phys. **101**, 2391 (1994); (d) J. T. Bendler and M. F. Schlesinger, J. Phys. Chem. **96**, 3970 (1992); (e) T. R. Kirkpatrick, D. Thirumalai, and P. G. Wolynes, Phys. Rev. A **40**, 1045 (1989); (f) Th. M. Nieuwenhuisen, Phys. Rev. Lett. **80**, 5580 (1998).

[3] (a) X. Cheng, D. Kivelson, and G. Tarjus, Phys. Rev. E **50**, 1711 (1994); (b) C. M. Roland and K. L. Ngai, J. Chem. Phys. **103**, 1152 (1995); **104**, 2967 (1996).

[4] (a) D. Sidebottom, R. Bergman, L. Börjesson, and L. M. Torell, Phys. Rev. Lett. **71**, 2260 (1993); (b) A. Brodin, L. Börjesson, D. Engberg, L. M. Torell, and A. P. Sokolov, Phys. Rev. B **53**, 11 511 (1996); (c) A. Patkowski, in *The Second International Discussion Meeting on Relaxations In Complex Systems*, edited by K. L. Ngai, E. Riande, and G. B. Wright [J. Non-Cryst. Solids **172–174**, 424 (1994)].

[5] S. N. Yannopoulos, G. N. Papatheodorou, and G. Fytas, Phys. Rev. E **53**, R1328 (1996).

[6] (a) B. J. Berne and R. Pecora, *Dynamic Light Scattering* (Wiley, New York, 1976); (b) J. P. Boon and S. Yip, *Molecular Hydrodynamics* (Dover, New York, 1991).

[7] G. Fytas and G. Meier, in *Dynamic Light Scattering. The Method and Some Applications*, edited by W. Brown (Oxford Science, New York, 1993), pp. 407–467, and references therein.

[8] (a) G. Li, W. M. Du, A. Sakai, and H. Z. Cummins, Phys. Rev. A **46**, 3343 (1992); (b) K. L. Ngai, G. Floudas, and A. K. Rizos, J. Chem. Phys. **106**, 6957 (1997).

[9] L. M. Torell, J. Chem. Phys. **76**, 3467 (1982); L. M. Torell and R. Aronsson, *ibid.* **78**, 1121 (1983).

[10] G. Li, W. M. Du, J. Hernandez, and H. Z. Cummins, Phys. Rev. E **48**, 1192 (1993).

[11] L. M. Torell, D. C. Ziegler, and C. A. Angell, J. Chem. Phys. **81**, 5053 (1984).

[12] D. Tielbürger, R. Merz, R. Ehrenfels, and S. Hunklinger, Phys. Rev. B **45**, 2750 (1996).

[13] M. Grimsditch, R. Bhadra, and L. M. Torell, Phys. Rev. Lett. **62**, 2616 (1989).

[14] J. Kieffer, Phys. Rev. B **50**, 17 (1994).

[15] H. E. G. Knape, J. Chem. Phys. **80**, 4788 (1984).

[16] H. Zhu, Y. Sato, T. Yamamura, K. Sugomoto, and Y. Sato, Ber. Bunsenges. Phys. Chem. **97**, 583 (1993).

[17] M. Soltwisch, J. Sukmanowski, and D. Quitmann, J. Chem. Phys. **86**, 3207 (1987).

[18] S. Loheider, G. Vögel, I. Petscheritzin, M. Soltwisch, and D. Quitmann, J. Chem. Phys. **93**, 5436 (1990).

[19] N. J. Tao, G. Li, and H. Z. Cummins, Phys. Rev. B **43**, 5815 (1991).

[20] S. N. Yannopoulos, Ph.D. thesis, University of Patras, 1996.

[21] S. N. Yannopoulos, G. D. Zissi, G. N. Papatheodorou, and G. Fytas (unpublished).

[22] C. Dreyfus, M. J. Lebon, H. Z. Cummins, J. Toulouse, B. Bonello, and R. M. Pick, Phys. Rev. Lett. **69**, 3666 (1992).

[23] W. M. Du, G. Li, H. Z. Cummins, M. Fuchs, J. Toulouse, and L. A. Knauss, Phys. Rev. E **49**, 2192 (1994).

[24] M. Fuchs, W. Götze, and A. Latz, Chem. Phys. **149**, 185 (1990).

[25] J. E. Masnik, J. Kieffer, and J. D. Bass, J. Am. Ceram. Soc. **76**, 3073 (1993).
[26] J. E. Masnik, J. Kieffer, and J. D. Bass, J. Chem. Phys. **103**, 9907 (1995).
[27] J. Kieffer, J. E. Masnik, O. Nickolayev, and J. D. Bass, Phys. Rev. B **58**, 694 (1998).
[28] C. C. Lai, P. B. Macedo, and C. J. Montrose, J. Am. Ceram. Soc. **58**, 120 (1975).
[29] E. A. Pavlatou, S. N. Yannopoulos, G. N. Papatheodorou, and G. Fytas, J. Phys. Chem. **101**, 8748 (1997).
[30] (a) E. A. Pavlatou, A. K. Rizos, G. N. Papatheodorou, and G. Fytas, J. Chem. Phys. **94**, 224 (1991); (b) D. L. Sidebottom and C. M. Sorensen, *ibid.* **91**, 7153 (1989).
[31] (a) J. A. Bucaro, H. D. Dardy, and R. D. Cosaro, J. Appl. Phys. **46**, 741 (1975); (b) D. L. Sidebottom, R. Bergman, L. Börjesson, and L. M. Torell, Phys. Rev. Lett. **71**, 2260 (1993).
[32] K. A. Becker, K. Plieth, and I. N. Stranski, Prog. Inorg. Chem. **4**, 1 (1962).
[33] O. Mazurin, *Handbook of Glass Data* (Elsevier, New York, 1987).
[34] M. Imaoka and H. Hasegawa, Phys. Chem. Glasses **21**, 67 (1980).
[35] (a) G. N. Papatheodorou and S. A. Solin, Solid State Commun. **16**, 5 (1974); (b) G. N. Papatheodorou and S. A. Solin, Phys. Rev. B **13**, 1741 (1976); (c) E. J. Flynn, S. A. Solin, and G. N. Papatheodorou, *ibid.* **13**, 1752 (1976); (d) E. Rytter, S. K. Goats, and G. N. Papatheodorou, J. Chem. Phys. **69**, 3717 (1978).
[36] (a) R. F. Pettifer and P. W. McMillan, Philos. Mag. **35**, 871 (1977); (b) S. J. Gurman and R. F. Pettifer, Philos. Mag. B **40**, 345 (1979).
[37] (a) F. L. Galeener, G. Luckovsky, and R. H. Geils, Phys. Rev. B **19**, 4251 (1979); (b) G. Luckovsky and F. L. Galeener, J. Non-Cryst. Solids **37**, 53 (1980).
[38] D. Beeman, R. Lynds, and M. R. Anderson, J. Non-Cryst. Solids **42**, 61 (1980).
[39] A. G. Clare, A. C. Wright, R. N. Sinclair, F. L. Galeener, and A. E. Geissberger, J. Non-Cryst. Solids **111**, 123 (1989).
[40] R. E. Strakna and H. T. Savage, J. Appl. Phys. **33**, 1445 (1964).
[41] I. Karutz and I. N. Stranski, Z. Anorg. Allg. Chem. **292**, 330 (1957).
[42] R. D. Mountain, J. Res. Natl. Bur. Stand., Sect. A **70**, 207 (1966); **72**, 95 (1968).
[43] M. Soltwisch, G. Ruocco, B. Balschun, J. Bosse, V. Mazzacurati, and D. Quitmann, Phys. Rev. E **57**, 720 (1998).
[44] R. Böhmer, K. L. Ngai, C. A. Angell, and D. J. Plazek, J. Chem. Phys. **99**, 4201 (1993).
[45] M. D. Ediger, C. A. Angell, and S. R. Nagel, J. Phys. Chem. **100**, 13 200 (1996).
[46] The reason for this, is that since Brillouin spectroscopy elucidates the GHz frequency range a relaxation time estimated at $T_{\max}$ through the relation $\omega_B \tau \sim 1$ is always found near the 10^{-11} s time. Consequently, a decrease in fragility corresponds to a shift of the $\tau(T_{\max})$ point on the left side of a fragility plot, following the narrow band close to 10^{-11} s. Thus, reaching to the strong limit, the $T_{\max}-T_g$ difference has to increase vividly.
[47] G. Monaco, D. Fioretto, C. Masciovecchio, G. Ruocco, and F. Sette, Phys. Rev. Lett. **82**, 1776 (1999).
[48] (a) P. W. Anderson, B. I. Halperin, and C. M. Varma, Philos. Mag. **25**, 1 (1972); (b) W. A. Phillips, J. Low Temp. Phys. **7**, 351 (1972).
[49] T. Gleim, W. Kob, and K. Binder, Phys. Rev. Lett. **81**, 4404 (1998).
[50] S. N. Yannopoulos, G. N. Papatheodorou, and G. Fytas, J. Chem. Phys. **107**, 1341 (1997).
[51] (a) U. Buchenau, C. Schönfeld, D. Richter, T. Kanaya, K. Kaji, and R. Wehrmann, Phys. Rev. Lett. **73**, 2344 (1994); (b) B. Frick and D. Richter, Phys. Rev. B **47**, 14 795 (1993).
[52] (a) O. L. Anderson and H. L. Bömmel, J. Am. Ceram. Soc. **38**, 125 (1955); (b) R. E. Strakna, Phys. Rev. **123**, 2020 (1961); (c) M. R. Vukcevich, J. Non-Cryst. Solids **11**, 25 (1972); (d) U. Buchenau, in *Dynamics of Disordered Materials*, edited by D. Richter, A. J. Dianoux, W. Petry, and J. Teixeira (Springer-Verlag, Berlin, 1989), Vol. 37, pp. 172–181, and references therein.
[53] A. Takada, C. R. A. Catlow, and G. D. Price, J. Phys.: Condens. Matter **7**, 8659 (1995); **7**, 8693 (1995).
[54] B. K. Vainshtein, V. M. Fridkin, and V. L. Indenbom, *Fundamentals of Crystals* (Springer-Verlag, Berlin, 1994).
[55] C. A. Angell, J. Non-Cryst. Solids **131-133**, 15 (1991).
[56] (a) J. T. Bendler and M. F. Shlesinger, J. Mol. Liq. **36**, 37 (1987); J. Stat. Phys. **53**, 531 (1988)
[57] E. W. Fischer, Physica A **201**, 183 (1994); A. S. Bakai, Low Temp. Phys. **22**, 733 (1996); **24**, 20 (1998).
[58] It should be noted here that the LP ratio values could be overestimated if parasitic light due to dust, etc., also contributes to the Rayleigh peak intensity. But even in the case where this contribution reaches the 50% of the ''pure'' elastic intensity, the T_C^{LP} value is limited in an interval of about 20 °C.
[59] (a) T. A. Vilgis, J. Phys.: Condens. Matter **2**, 3667 (1990); Phys. Rev. B **47**, 2882 (1993).
[60] R. Zallen, *Physics of Amorphous Solids* (Wiley, New York, 1983).
[61] H. Bässler, Phys. Rev. Lett. **58**, 767 (1987).
[62] (a) G. Meier, F. Kremer, G. Fytas, and A. K. Rizos, J. Polym. Sci., Part B: Polym. Phys. **34**, 1391 (1996); (b) G. Floudas, P. Placke, P. Stepanek, W. Brown, G. Fytas, and K. L. Ngai, Macromolecules **28**, 6799 (1995).
[63] E. W. Fischer, E. Donth, and W. Steffen, Phys. Rev. Lett. **68**, 2344 (1992).
[64] (a) K. Schmidt-Rohr and H. W. Spiess, Phys. Rev. Lett. **66**, 3020 (1991); (b) A. Heuer, M. Wilhelm, H. Zimmermann, and H. W. Spiess, *ibid.* **75**, 2851 (1995).
[65] J. C. Phillips, J. Non-Cryst. Solids **172-174**, 98 (1994).
[66] H. Maekawa, Y. Inagaki, S. Shimokawa, and T. Yokokawa, J. Chem. Phys. **103**, 371 (1995).